

PACS 78.66.-w, 81.15.Cd, Dj

Comparison of optical properties of TiO₂ thin films prepared by reactive magnetron sputtering and electron-beam evaporation techniques

V.V. Brus¹, Z.D. Kovalyuk¹, O.A. Parfenyuk², N.D. Vakhnyak³

¹*Frantsevich Institute for Problems of Materials Science, NAS of Ukraine, Chernivtsi Branch, 5, Iryna Vilde str., 58001 Chernivtsi, Ukraine; E-mail: victorbrus@mail.ru*

²*Yu. Fedkovych Chernivtsi National University, 2, Kotsyubynsky str., 58012 Chernivtsi, Ukraine; E-mail: o.parfenyuk@chnu.edu.ua*

³*V. Lashkaryov Institute of Semiconductor Physics, NAS of Ukraine, 41, prospect Nauky, 03028 Kyiv, Ukraine; E-mail: div47@isp.kiev.ua*

Abstract. The envelope method was used to determine optical constants of TiO₂ thin films deposited by DC reactive magnetron sputtering and electron-beam evaporation techniques. The density and thickness of the thin films were calculated. Optical properties of the TiO₂ thin films were strongly dependent on the deposition technology. The TiO₂ thin films prepared by magnetron sputtering and electron-beam evaporation methods were established to be indirect band semiconductors with the band gap energies 3.15 and 3.43 eV, respectively.

Keywords: TiO₂, thin film, transmittance, optical properties.

Manuscript received 16.06.11; revised manuscript received 10.08.11; accepted for publication 14.09.11; published online 30.11.11.

1. Introduction

During the recent decade, titanium dioxide has been one of the most promising materials among transparent, conductive oxides. Today, many researches are interested in TiO₂ thin films and their application in different optical and photoelectrical devices. TiO₂ thin film can be efficiently applied in antireflective coatings, optical filters, wide band gap “windows” for solar cells, etc., due to their high transparency for visible light, large value of refractive index, controllable specific electric resistance and good chemical resistance [1–3].

A number of techniques are used for preparation of TiO₂ thin films, in particular, magnetron sputtering, electron-beam evaporation, spray pyrolysis, etc.

It is worth noting that the structure, optical and electrical properties of TiO₂ thin films are strongly dependent on deposition technology.

The optical properties of TiO₂ thin films prepared by two techniques: DC reactive magnetron sputtering (TiO₂(M) thin films) and electron-beam evaporation (TiO₂(EB) thin films) techniques have been compared in this work. The envelope method was used to analyze

transmission spectra with peaks and valleys induced by interference effects in thin films for evaluating their optical constants: refractive index $n(\lambda)$, absorption coefficient $\alpha(\lambda)$ and extinction coefficient $k(\lambda)$ [4–7].

2. Experimental details

The TiO₂(M) and TiO₂(EB) thin films were deposited onto cover glass substrates in an universal coating system “Laybold-Heraeus L560” using DC reactive magnetron sputtering and electron-beam evaporation techniques, respectively.

Before starting the deposition processes, the vacuum chamber was pumped down to a residual pressure of $5 \cdot 10^{-5}$ mbar.

For deposition of TiO₂(M) thin film, the titanium target (99.99%), a cylinder 100 mm in diameter and 5 mm thick, was mounted, on the magnetron table under water cooling and 7 cm from the substrates.

A short-term sputter-cleaning of the target and substrates by Ar ions was applied to eliminate the surface contaminants.

The mixture of pure argon and oxygen in the desirable ratio was prepared using two separate sources.

During the deposition process, the partial pressures of argon and oxygen were equal to $5 \cdot 10^{-3}$ and $2 \cdot 10^{-4}$ mbar, respectively. The set up magnetron power was 350 W. The deposition process lasted 20 min.

The $\text{TiO}_2(\text{EB})$ thin film deposition was carried out by electron-beam evaporation of pressed and sintered pellets from titanium dioxide powder (99.99%) with anatase structure. The pellets (9 mm in diameter) were pressed by a hydraulic press under a pressure of 3000 kilos/cm². This pressure was enough to provide the desirable mechanical strengths of the pellets for further technological operations. The pellets were sintered in air at 700 °C for 5 hours.

The electron beam intensity, deposition rate and film thicknesses were controlled by means of an INFICON XTC deposition controller.

It is worth noting that any additional heating of the substrates was not applied in either of the techniques. The equilibrium temperatures of the substrates induced by the technological heat for the magnetron sputtering and electron-beam evaporation processes were 200 °C and 100 °C, respectively.

The transmission spectra of $\text{TiO}_2(\text{M})$ and $\text{TiO}_2(\text{EB})$ thin films were obtained by means of a conventional spectrophotometer. The experimental data were measured within the range of wavelengths from 200 up to 1100 nm with 1 nm step.

3. Results and discussion

Fig. 1 shows the transmission spectrum of a clean glass substrate and that of the $\text{TiO}_2(\text{M})$ thin film – substrate and $\text{TiO}_2(\text{EB})$ thin film – substrate combinations. It is easy to see that the glass substrate remains entirely transparent near the intrinsic absorption edge of the TiO_2 thin films. This condition provides an unambiguous interpretation of the results of the experiment. Additionally, the transmission spectra of the TiO_2 thin films possess periodic peaks and valleys induced by interference effects indicating a high structural perfection of these thin films.

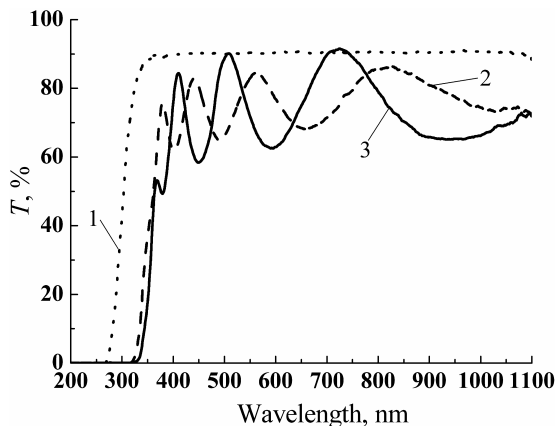


Fig. 1. Transmission spectra of the clean glass substrate (1), $\text{TiO}_2(\text{EB})$ thin film – substrate combination (2), $\text{TiO}_2(\text{M})$ thin film – substrate combination (3).

The optical properties of a thin film (refractive index $n(\lambda)$, absorption coefficient $\alpha(\lambda)$, extinction coefficient $k(\lambda)$ and thickness d) can be easily evaluated from a transmission spectrum with interference effects using the envelope method [4–7]. This method is applicable in the case of a weakly absorbing thin film on an entirely transparent substrate that is much thicker than the thin film. It is worth noting that these conditions are met in this work.

The envelope curves $T_{\max}(\lambda)$ and $T_{\min}(\lambda)$ form the foundation of the envelope method. They can be obtained by means of parabolic extrapolation of experimentally determined points that correspond with the location of interference maxima and minima (Fig. 2).

Having obtained the envelope curves, the refractive index $n(\lambda)$ of the TiO_2 thin films can be calculated with the following equation:

$$n(\lambda) = \left[\left(\frac{2n_s(T_M(\lambda) - T_m(\lambda))}{T_M(\lambda)T_m(\lambda)} + \frac{n_s^2 + 1}{2} \right) + \sqrt{\left(\frac{2n_s(T_M(\lambda) - T_m(\lambda))}{T_M(\lambda)T_m(\lambda)} + \frac{n_s^2 + 1}{2} \right)^2 - n_s^2} \right]^{\frac{1}{2}} \quad (1)$$

Here, n_s is the refractive index of the substrate:

$$n_s = \frac{1}{T_s} + \sqrt{\frac{1}{T_s^2} - 1}, \quad (2)$$

where T_s is the substrate transmittance in the transparent zone. For the cover glass substrate $T_s = 0.91$ (Fig. 1), hence following the equation (2) $n_s = 1.554$.

It should be emphasized that equation (1) is valid only within the interference zone. Outside this zone, the refractive index can be determined using an extrapolation of calculated data [5].

As one can see from Fig. 3, the refractive index, $n(\lambda)$, of the $\text{TiO}_2(\text{M})$ thin film is essentially larger than that of the $\text{TiO}_2(\text{EB})$ thin film. The increase in the refractive indexes at wavelengths $\lambda < 500$ nm corresponds to the decrease in transparency near the edge of intrinsic absorption in the TiO_2 thin films.

The linear relationship between the density and the refractive index of a TiO_2 thin film can be expressed as follows:

$$\rho = \frac{n(550) - 0.91933}{0.42751}, \quad (3)$$

where ρ is the density of a TiO_2 thin film (g/cm³) and $n(550)$ is the refractive index of a TiO_2 thin film at the wavelength $\lambda = 550$ nm [8].

The refractive index of the $\text{TiO}_2(\text{M})$ thin film and that of the $\text{TiO}_2(\text{EB})$ thin film at the wavelength 550 nm is equal to 2.51 and 2.23, respectively (Fig. 3). The density of the $\text{TiO}_2(\text{M})$ and $\text{TiO}_2(\text{EB})$ thin films calculated from the equation (3) is equal to 3.72 and 3.06 g/cm³, respectively.

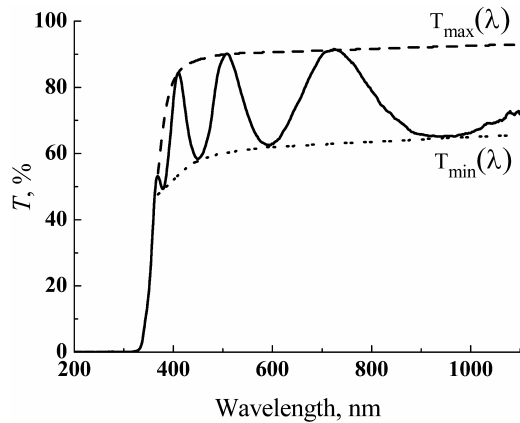


Fig. 2. The transmission spectra of the $\text{TiO}_2(\text{M})$ thin film with the envelope curves $T_{\max}(\lambda)$ and $T_{\min}(\lambda)$.

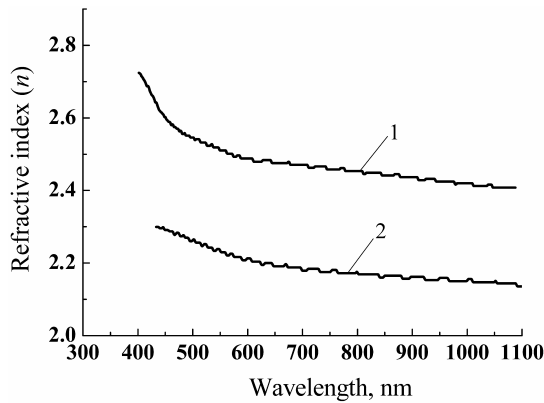


Fig. 3. The dependence of the refractive index n as a function of the wavelength λ for $\text{TiO}_2(\text{M})$ (1) and $\text{TiO}_2(\text{EB})$ (2) thin films.

The difference in the refractive indexes and densities of the $\text{TiO}_2(\text{M})$ and $\text{TiO}_2(\text{EB})$ thin films is caused by the higher kinetic energy inherent to thin film deposition by magnetron sputtering compared to the electron-beam evaporation technique. The deposition process with a higher kinetic energy results in a higher density as well as higher refractive index.

Following the envelope method, the next step is to calculate the thickness of the film:

$$d = \frac{A \lambda_1 \lambda_2}{2[n(\lambda_1)\lambda_2 - n(\lambda_2)\lambda_1]}, \quad (4)$$

where λ_1 and λ_2 are the wavelengths that correspond to adjacent extreme points in the transmission spectrum, $A = 1$ for two matching adjacent extremes, and $A = 0.5$ for two non-matching adjacent extremes. The values of the $\text{TiO}_2(\text{M})$ and (EB) films' thicknesses were calculated using the equation (4) for all combinations of adjacent extremes and were averaged, resulting in $d_{(\text{M})} = 0.315 \mu\text{m}$ and $d_{(\text{EB})} = 0.385 \mu\text{m}$.

The absorption coefficients of the $\text{TiO}_2(\text{M})$ and $\text{TiO}_2(\text{EB})$ thin films can be evaluated from the following equation:

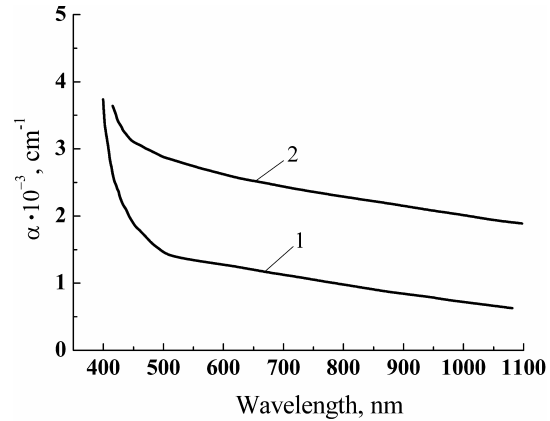


Fig. 4. The dependence of the absorption coefficient α as a function of the wavelength λ for $\text{TiO}_2(\text{M})$ (1) and $\text{TiO}_2(\text{EB})$ (2) thin films.

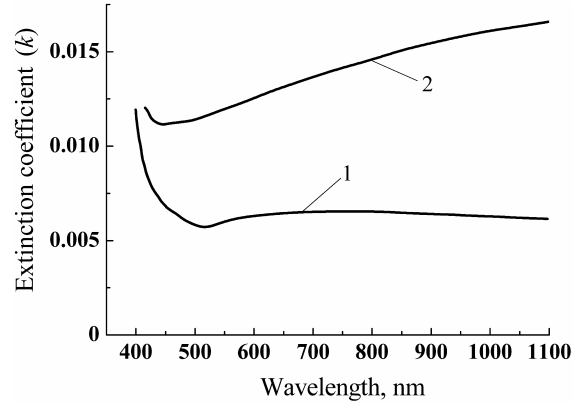


Fig. 5. The dependence of the extinction coefficient k as a function of the wavelength λ for $\text{TiO}_2(\text{M})$ (1) and $\text{TiO}_2(\text{EB})$ (2) thin films.

$$\alpha(\lambda) = \frac{1}{d} \ln \left[\frac{(n(\lambda)-1)(n(\lambda)-n_s) \left[\left(\frac{T_M(\lambda)}{T_m(\lambda)} \right)^{\frac{1}{2}} + 1 \right]}{(n(\lambda)+1)(n(\lambda)+n_s) \left[\left(\frac{T_M(\lambda)}{T_m(\lambda)} \right)^{\frac{1}{2}} - 1 \right]} \right]. \quad (5)$$

Fig. 4 shows the absorption coefficient $\alpha(\lambda)$ as a function of the wavelength for both of TiO_2 thin films. One can see an abrupt increase of the absorption coefficients in short wavelength regions near the intrinsic absorption edges of the $\text{TiO}_2(\text{M})$ and $\text{TiO}_2(\text{EB})$ thin films as well as a smooth decrease of the absorption coefficients as the wavelength increases ($\lambda > 500 \text{ nm}$). Finally, the extinction coefficient $k(\lambda)$ can be calculated from the following equation $k(\lambda) = \frac{\lambda \alpha(\lambda)}{4\pi}$ (Fig. 5). It is

seen in the figure that the extinction coefficients also abruptly increase near the intrinsic absorption edges of the TiO_2 thin films. It is interesting that the extinction coefficient of the $\text{TiO}_2(\text{EB})$ thin film, as opposed to the absorption coefficient of the $\text{TiO}_2(\text{M})$, rises linearly

within the transparent region ($\lambda > 500$ nm) as the wavelength increases.

The envelope method can be applied only in the high transparency region of a thin film. Since the following conditions are true in the narrow wavelength region ($330 < \lambda < 400$ nm): strong absorption in the TiO₂ thin film, the entirely transparent substrate and $n(\lambda)^2 \gg k(\lambda)^2$, the absorption coefficient $\alpha(\lambda)$ ($330 < \lambda < 400$ nm) of the TiO₂ thin film can be determined from the following equation [10]:

$$\alpha(\lambda) = \frac{1}{d} \ln \left[\frac{(1 - R_1(\lambda))(1 - R_2(\lambda))(1 - R_{12}(\lambda))}{T(\lambda)} \right], \quad (6)$$

where $T(\lambda)$ is the optical transmittance, $R_1(\lambda)$, $R_2(\lambda)$ and $R_{12}(\lambda)$ are the reflection coefficients for the following interfaces: air – TiO₂ thin film, TiO₂ thin film – substrate, substrate – air. Assuming that $n(\lambda)^2 \gg k(\lambda)^2$ the reflection coefficients can be expressed by the following equations:

$$R_1(\lambda) = \left(\frac{n(\lambda) - 1}{n(\lambda) + 1} \right)^2, \quad R_2(\lambda) = \left(\frac{1 - n_s}{1 + n_s} \right)^2,$$

$$R_{12}(\lambda) = \left(\frac{n_s - n(\lambda)}{n_s + n(\lambda)} \right)^2.$$

The absorption coefficient of the TiO₂(M) and TiO₂(EB) thin films were analyzed by equation (7) in the fundamental absorption zone of the thin films:

$$\alpha h\nu = B(h\nu - E_g)^2, \quad (7)$$

where B is the constant that possesses different values for TiO₂(M) and TiO₂(EB) thin films. This dependence of $\alpha h\nu$ on $h\nu$ provides evidence that the TiO₂ thin films deposited by DC reactive magnetron sputtering and electron-beam evaporation methods are indirect band semiconductors. Also, the band gap energies of TiO₂(M) and TiO₂(EB) thin films were determined by the interception of an extrapolated linear sections of the appropriate $(\alpha h\nu)^{1/2}$ vs $h\nu$ curves with the photon energy axis (Fig. 6). The resultant values of the band gap energies $E_{g(M)} = 3.15$ eV and $E_{g(EB)} = 3.43$ eV, respectively, are well correlated with the reported data [9, 11].

Taking into account the small density (3.06 g/cm³) and large value of the band gap energy ($E_{g(EB)} = 3.43$ eV), the TiO₂(EB) thin film may be considered as consisting mainly of an amorphous phase [8, 12]. The amorphous phase can be induced by the low temperature (100 °C) during the thin film deposition. It is quite obvious that this suggestion must be checked experimentally.

¹ TiO₂ is an indirect band semiconductor (relatively small value of the extinction coefficient k) with the largest value of the refractive index among transparent conductive oxides [9]. That is why the inequality $n(\lambda)^2 \gg k(\lambda)^2$ is valid even within the strong absorption zone of a TiO₂ thin film.

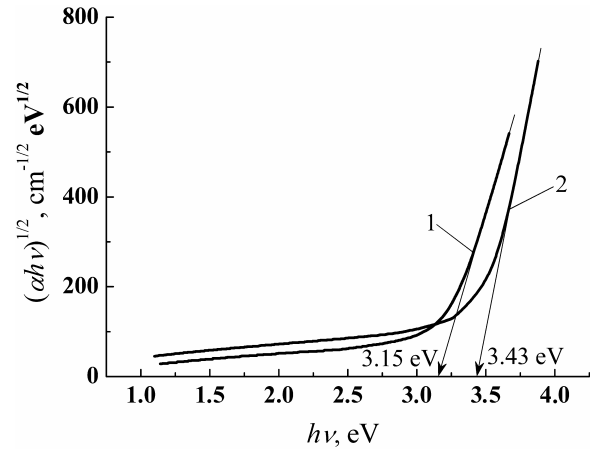


Fig. 6. The dependence $(\alpha h\nu)^{1/2}$ vs $h\nu$ for TiO₂(M) (1) and TiO₂(EB) (2) thin films.

4. Conclusions

TiO₂ thin films were deposited onto cover glass substrates by DC reactive magnetron sputtering and electron-beam evaporation techniques.

The transmission spectra of TiO₂(M) and TiO₂(EB) thin films were measured within the wavelength range from 200 up to 1100 nm with 1-nm step. The transmission spectra of the TiO₂ thin films possess periodic peaks and valleys induced by interference effects. The envelope method was employed to determine the thickness d and optical properties of the thin films, in particular, the refractive index $n(\lambda)$, the absorption coefficient $\alpha(\lambda)$ and extinction coefficient $k(\lambda)$ as the functions of the wavelength. The densities of TiO₂(M) and TiO₂(EB) thin films were calculated to be 3.72 and 3.05 g/cm³, respectively.

The TiO₂(M) and TiO₂(EB) thin films were established to be indirect band gap semiconductors with the band gap energies 3.15 and 3.43 eV, respectively.

References

1. U. Diebold, The surface science of titanium dioxide // *Surf. Sci. Repts.* **43**, p. 53-229 (2003).
2. M. Barrera, J. Pla, C. Bocchi, A. Migliori, Antireflecting-passivating dielectric films on crystalline silicon solar cells for space applications // *Solar Energy Materials & Solar Cells* **92**, p. 1115-1122 (2008).
3. K. Ernst, A. Belaidi, R. Konenkamp, Solar cell with extremely thin absorber on highly structured substrate // *Semicond. Sci. Technol.* **18**, p. 475-479 (2003).
4. R. Swanepoel, Determination of the thickness and optical constants of amorphous silicon // *J. Phys. E: Sci. Instrum.* **16**, p. 1214-1222 (1983).
5. J. Sanchez-Gonzalez, A. Diaz-Parralejo, A.L. Ortiz, Determination of optical properties in nanostructured

- thin films using the Swanepoel method // *Appl. Surf. Sci.* **252**, p. 6013-6017 (2006).
6. S. Ilican, M. Gaglar, Y. Gaglar, Determination of the thickness and optical constants of transparent indium-doped ZnO thin films by the envelope method // *Materials Science – Poland*, **25**, p. 709-718 (2007).
 7. C. Gumus, O.M. Ozkendir, H. Kavak, Y. Ufuktepe, Structural and optical properties of zinc oxide thin films prepared by spray pyrolysis method // *J. Optoelectron. Adv. Mater.* **8**, p. 299-303 (2006).
 8. A. Bendavid, P.J. Martin, H. Takikawa, Deposition and modification of titanium dioxide thin films by filtered arc deposition // *Thin Solid Films*, **360**, p. 241-249 (2000).
 9. B. Karunakaran, R.T. Rajendra Kumar, C. Viswanathan, D. Mangalaraj, Sa.K. Narayandass, G. Mohan Rao, Optical constants of DC magnetron sputtered titanium dioxide thin films measured by spectroscopic ellipsometry // *Crystal. Res. Technol.* **38**, pp. 773-778 (2003).
 10. Yu.I. Ukhonov, *Optical Properties of Semiconductors*. Nauka, Moscow, 1977 (in Russian).
 11. P. Eiamchai, P. Chindaudom, A. Pokaipisit, P. Limsuwan, A spectroscopic ellipsometry study of TiO₂ thin films prepared by ion-assisted electron-beam evaporation // *Current Appl. Phys.* **9**, p. 707-712 (2009).
 12. P. Lobl, M. Huppertz, D. Mergel, Nucleation and growth in TiO₂ films prepared by sputtering and evaporation // *Thin Solid Films*, **251**, p. 72-79 (1994).